Tilt prior to explosions and the effect of topography on ultra-long-period seismic records at Fuego volcano, Guatemala

John J. Lyons,[1] Gregory P. Waite,[2] Mie Ichihara,[3] and Jonathan M. Lees[4]

Received 3 February 2012; revised 21 March 2012; accepted 27 March 2012; published 24 April 2012.

[1] Ground tilt is measured from broadband seismic records prior to frequent explosions at Fuego volcano, Guatemala. We are able to resolve tilt beginning 20–30 minutes prior to explosions, followed by a rapid reversal in deformation coincident with explosion onsets. The tilt amplitude and polarity recorded on the horizontal channels vary from station to station such that the steep and unusual topography of the upper cone of Fuego appears to affect the ultra-long-period signals. We account for the effect of topography and attempt to constrain the tilt source depth and geometry through finite-difference modeling. The results indicate a shallow spherical pressure source, and that topography must be considered when attempting to model tilt sources at volcanoes with steep topography. The tilt signals are interpreted as pressurization of the shallow conduit beneath a crystallized plug followed by elastic deflation concurrent with explosive pressure release. **Citation:** Lyons, J. J., G. P. Waite, M. Ichihara, and J. M. Lees (2012), Tilt prior to explosions and the effect of topography on ultra-long-period seismic records at Fuego volcano, Guatemala, *Geophys. Res. Lett.*, *39*, L08305, doi:10.1029/2012GL051184.

1. Introduction

[2] The dynamics of small (VEI < 2), transient volcanic explosions are increasingly becoming better understood through the use of broadband seismometers, which allow for investigation of signals over a wide range of timescales. Very-long-period (VLP) signals have been used to image conduit geometry and unravel the source mechanisms of strombolian and vulcanian explosions, and these studies typically make use of signals as low as the natural period of the instrument [e.g., *Chouet et al.*, 2003; *Dawson et al.*, 2011; *Lyons and Waite*, 2011; *Waite et al.*, 2008]. Several studies have extended the timescale of observation beyond the low corner of portable seismic sensors to investigate small ground rotation signals accompanying short-lived explosions that can be extracted from the horizontal components of broadband sensors [*Aoyama and Oshima*, 2008; *Genco and Ripepe*, 2010; *Wielandt and Forbriger*, 1999]. The ability to recover information about ground displacement and tilt with a single instrument greatly improves the understanding of volcanic eruptions, particularly in places where more permanent installations of dedicated tilt sensors are impossible.

[3] Inflation – deflation sequences related to slow accumulation of pressure and explosive degassing have been well-documented using tiltmeters and broadband seismometers for large eruptions at Soufriere Hills [*Voight et al.*, 1999], Merapi [*Voight et al.*, 2000], and Anatahan [*Wiens et al.*, 2005]. However, similar sequences over shorter timescales have also been extracted from broadband seismic records of strombolian explosions [*Genco and Ripepe*, 2010; *Wielandt and Forbriger*, 1999]. In other cases, tilt from broadband sensors recorded deflations associated with phreatic explosions at Meakan-dake [*Aoyama and Oshima*, 2008] and small pyroclastic explosions at Santiaguito [*Johnson et al.*, 2009; *Sanderson et al.*, 2010]. In each case, the timescale and pattern of deformation accompanying explosions facilitated the interpretation of eruption dynamics, especially when recorded in conjunction with other remote sensing data.

[4] In this paper, we report observations of tilt recorded on broadband seismometers associated with explosions from Fuego volcano, Guatemala, recorded over 20 days in January 2009. Fuego is a 3800 m stratovolcano that regularly produces strombolian and weak vulcanian explosions, observed on a temporary network of broadband seismic (Güralp CMG-3ESPC and CMG-40T sensors, 60 and 30 s corners, respectively) and infrasound sensors (All Sensors differential pressure transducers, 0.001–50 s) deployed 800 m to 2 km from the summit crater (Figure 1a). The strongest recorded explosions generated impulsive infrasound and seismic signals, ejected incandescent bombs and tephra, and were associated with repetitive VLP seismicity. A waveform inversion of a VLP event locates the source centroid 300 m west and 300 m below the level of the summit crater, and the source mechanism is interpreted to be an inflation-deflation-reinflation cycle in a shallowly dipping sill [*Lyons and Waite*, 2011].

[5] The stations that most reliably recorded tilt were located on the steep upper flanks and prominent ridge extending to the north (Figure 1a). The correlation between varying tilt polarity and amplitude on the horizontal channels, and the sensor location suggests the topography influences the tilt signal. Effects of topography on tilt signals have been modeled numerically [e.g., *Cayol and Cornet*, 1998; *McTigue and Segall*, 1988; *Rodgers*, 1968], but we are unaware of other datasets that display this effect at active volcanoes. Modeling of the topographic influence and constraints on the depth and geometry of the tilt source were acquired with the three-dimensional (3D) finite-difference method of *Ohminato and Chouet* [1997], including the 3D topography of Fuego that includes a prominent ridge extending north from the otherwise conical edifice. The tilt signals are interpreted as inflation of the shallow conduit due to pressurization beneath a crystallized plug followed by rapid deflation concurrent with the onset of explosions, and

[1]Instituto Geofisico, Escuela Politecnica Nacional, Quito, Ecuador.
[2]Department of Geological Engineering and Sciences, Michigan Technological University, Houghton, Michigan, USA.
[3]Earthquake Research Institute, University of Tokyo, Tokyo, Japan.
[4]Department of Geological Sciences, University of North Carolina at Chapel Hill, Chapel Hill, North Carolina, USA.

0094-8276/12/2012GL051184

model results show that topography must be considered in attempts to constrain source depth and geometry on steep volcanoes.

2. Tilt Data

[6] The horizontal components of broadband seismometers are sensitive to tilt through gravitational acceleration. *Rodgers* [1968] characterized the effect of tilting on inertial seismometers and described the relationship between displacement and tilt as a function of angular frequency. A recent experiment by *Aoyama and Oshima* [2008] confirms that the horizontal components of modern force-feedback broadband seismometers are also susceptible to tilt. The broadband signal is more susceptible to tilt with increasing period so that tilt dominates translation at periods below the sensor corner if the seismometer experiences substantial rotation [*Wielandt and Forbriger*, 1999]. The tilt transfer function of a broadband sensor is calculated from the velocity transfer function specified by the manufacturer for a given instrument [*Aoyama and Oshima*, 2008]. Tilts associated with relatively weak strombolian and vulcanian explosions can be quite small, but some tilt signal can still be recovered from the broadband record using the tilt transfer function [*Aoyama and Oshima*, 2008; *Genco and Ripepe*, 2010]. The tilt transfer function of the CMG-40T and CMG-3ESPC sensors below the natural frequency is approximately proportional to the frequency. This allows the tilt time series $\tau(t)$ to be calculated from a time integral of the output voltage of the seismometer $p(t)$ by (equation (23) in Text S1 in the auxiliary material [*Aoyama*, 2008]):[1]

$$\tau(t) = -\frac{S\omega_0^2}{g}\int p(t)dt \qquad (1)$$

where S is the seismometer sensitivity, g is the gravitational acceleration, and ω_0 is the natural angular frequency. Strictly, (1) includes the effect of the translational acceleration of the ground (Text S1), but its contribution is regarded as negligible in the very low frequency of interest.

[7] We extract the tilt signal in four steps by 1) removing the mean, 2) integrating the instrument output, 3) low-pass filtering below the natural frequency of the instrument, and 4) multiplying by $-\frac{S\omega_0^2}{g}$. Positive east and north components of tilt are defined as tilt down to the east and north, respectively.

[8] The tilt signals were weak (nanoradians) and this method of extracting tilt can be controversial because a long-period signal before a high-amplitude impulse can be an

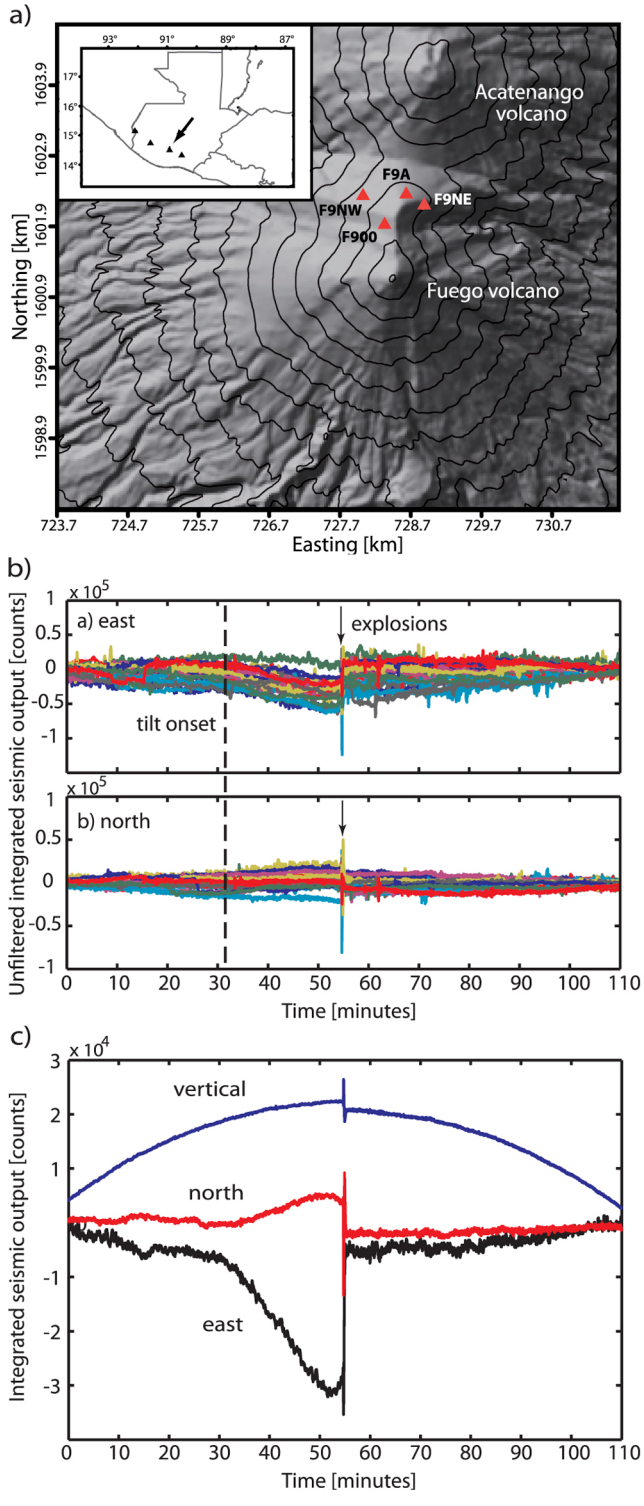

Figure 1. (a) Digital elevation model of Fuego volcano indicating the locations of the broadband seismic stations that recorded a tilt signal associated with explosions in January 2009. The stations were installed on the steep topography (>30°) and prominent ridge extending north from the summit of Fuego. Contour interval is 200 m. (b) Unfiltered integrated seismometer output for 24 explosions recorded at station F900. The sensor response was not deconvolved in order to simplify the interpretation. Instrument drift and other high-frequency noise produce significant variation in the traces but a clear, consistent trend occurs at ~31 minutes (vertical dashed line) that indicates the onset of a coherent tilt signal. The impulsive explosions occur at 55 minutes (arrow), more than 20 minutes after the initial tilt signal. (c) Unfiltered integrated seismometer output stacks of the 24 explosions from Figure 1b. The tilt signal clearly starts at ~31 minutes in the north and east channel, while the vertical channel only records instrument drift until the explosions occurs at 55 minutes.

[1] Auxiliary materials are available in the HTML. doi:10.1029/2012GL051184.

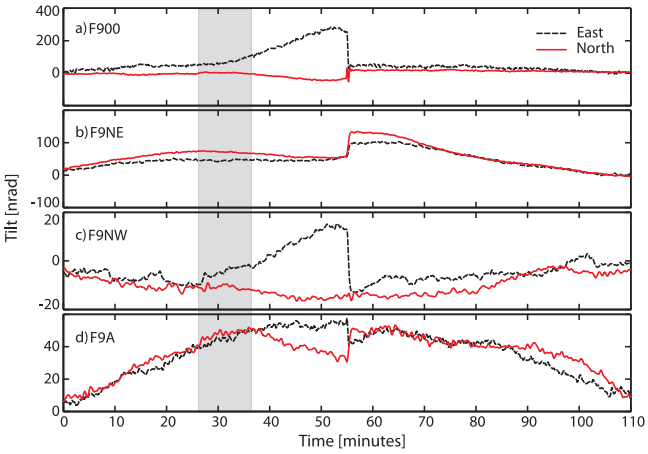

Figure 2. Stacks of tilt signals preceding explosions at stations F900 (24 events), F9NE (12 events), F9NW (14 events), and F9A (29 events). The gray box indicates the span of tilt onsets at the different stations. Instrument drift is clear in all the stations except F900 due to the low amplitude of the tilt signal at the stations further from the summit. Tilt begins ~20–30 minutes before the explosion onset (at minute 55).

artifact of low-pass, acausal filtering. To investigate this, we apply the above steps 1) and 2) to full sample-rate, unfiltered seismic record in windows centered on the times of known explosions that produced an infrasound pulse of >100 Pa at station F900. The station nearest the vent, F900, has the highest signal-to-noise ratios, and a consistent trend emerges in the unfiltered time integrated traces when the events are plotted together (Figure 1b). This is unequivocal evidence that a repetitive signal is recorded ~20–30 minutes prior to the explosions that is certainly not a filter or signal processing artifact. Stacking all the traces in Figure 1b shows a clear, consistent signal prior to the explosions (Figure 1c). Because the signal exists in the horizontal components, but not in the vertical component, and the time scale is much longer than the natural period of the seismometer, it is regarded as tilt signal and not displacement or instrument drift.

[9] The filtering for step 3) is performed in two phases in order to avoid aliasing and achieve an acceptable filter order. The full-sample rate integrated signal is first low-pass filtered below 0.1 Hz and decimated to 10 sps, then it is low-pass filtered below the natural frequency of the instrument (40T = F900, F9A; 3ESPC = F9NE, F9NW). A single pass, causal filter was used in order to avoid any spurious features sometimes caused by acausal filters (MATLAB filter routine included in Text S2). However, an acausal filter was also used to investigate filter artifacts and we found that when following this signal processing routine, minimal changes to the tilt signals were introduced. The tilt onset times vary from ~20–30 minutes prior to the explosion onset, with earlier onsets recorded at the stations with 60 s instruments, possibly indicating greater sensitivity to longer period tilt. The strength of the tilt signal decreases rapidly with distance, but through stacking coherent signal is detected at the four closest stations (Figure 2). Using a simple signal-to-noise evaluation to discard especially noisy traces, the stacked waveforms in Figure 2 consist of 24, 12, 14, and 29 events for stations F900, F9NE, F9NW, and F9A, respectively.

[10] Any estimate of tilt source depth and geometry at Fuego must include the topography of the upper edifice because slopes are typically >30° in the study area and irregular, with a sharp north-south trending ridge that extends north from the summit and terminates in a steep north-facing slope (Figure 1a). The variation in amplitude and tilt polarity on the horizontal channels at different station locations on this topography is striking (Figure 2). East down tilt dominates at F900 and F9NW, while F9A displays only south down motion and F9NE shows mostly south down tilt, with a minor east component. While it is possible that individual site effects, inhomogeneous substrate strength, or a complicated pressurizing geometry could cause this relationship, the systematic variation in polarity with station location on the steep and irregular topography of Fuego is a more likely candidate.

3. Modeling the Tilt Source

[11] Volcanic deformation is often modeled using analytical solutions to either an isotropic volumetric point source [*Mogi*, 1958] or an Okada dislocation surface (dike or sill) [*Okada*, 1985] due to the simplicity of these models and the ease of implementation. However, these models do not incorporate topography which has been shown to have a strong effect on the deformation field, particularly for slopes above 20° [*Cayol and Cornet*, 1998; *Meo et al.*, 2008], and neither of these models are able to replicate the tilt signals we recorded. Based on these results, we choose to include the 3D topography in forward models of the tilt signal through the finite-difference method of *Ohminato and Chouet* [1997]. Our model space is centered at the summit of Fuego and extends 12 km east–west, 9 km north–south and 6 km in the vertical, with 40 m grid spacing. A homogeneous velocity model is used because the velocity profile of Fuego is unknown. The compressional wave velocity is 3.5 km/s, shear wave velocity is 2 km/s, and density is 2650 kg/m^3. Synthetic Green functions of the curl of the displacement field (equal to twice the tilt) are generated with the finite-difference code. Green functions are convolved with a 20 s cosine stabilizing function that has energy in periods longer than 10 s. While much longer-duration source-time functions were tested, this 20 s signal produced synthetic rotations with the same simple shape and amplitude, thus decreasing computing time and increasing the number of source locations considered.

[12] All potential sources were modeled as inflating (i.e., pressurizing) based on our observations of the explosions and seismic, gas, and infrasound data. SO_2 emissions show a slow decline for tens of minutes prior to explosions, followed by increased flux following explosions, which is interpreted as sealing of the conduit followed by explosive release of overpressure [*Nadeau et al.*, 2011]. Modeling of the VLP seismic signals associated with explosive events at Fuego also suggests shallow conduit inflation just prior to explosions, and the explosion infrasound indicates large overpressures had developed in the shallow conduit [*Lyons and Waite*, 2011]. A pressurized, inflating source is also supported by observations of explosions that produced abundant incandescent bombs and strong audible reports.

[13] Three potential source geometries are considered: single pipes, single cracks, and spherical sources. The pipe

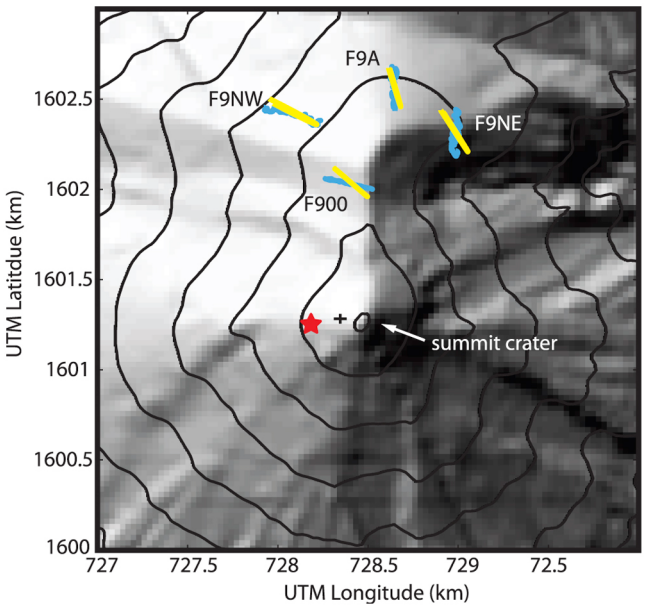

Figure 3. Pre-explosion tilt particle motions plotted at the station locations on a DEM of Fuego's upper cone. Blue traces are the stacked data and yellow traces are the best synthetic spherical source. Amplitudes are normalized by station. The red star represents the location of the VLP seismicity from *Lyons and Waite* [2011] and the black cross is the best-fit tilt source. Contour intervals are 200 m.

and crack moment tensors are generated using equations (15) and (16) of *Chouet* [1996], assuming a Poisson ratio of 1/3. Although some information about the geometry of the conduit is available from the VLP waveform inversion of *Lyons and Waite* [2011], we initially vary azimuth in 15° intervals and plunge in 30° over all possible crack and pipe orientations for source locations extending 500 m west, 100 m east, 300 m north–south and 1000 m below the summit crater.

3.1. Model Results

[14] Rather than performing a full-waveform inversion, we choose to simply compare the tilt directions of the real data and synthetics. As discussed in the previous section, there are subtle differences in the tilt waveforms between the 60 s and 30 s sensors, which hint at possible errors in the tilt estimates. Quantifying the uncertainty in absolute tilt values for different types of broadband seismometers is beyond the scope of this study. However, reasonably consistent values are expected from both horizontal channels of the same sensor, meaning the ratio of the two channels should be reliable. Therefore pre-explosion tilt "particle motions" rather than the whole waveform were chosen for modeling. The results are compared by determining the direction of maximum tilt from the real and synthetic data and calculating the RMS error for each station:

$$\sqrt{\left(\frac{1}{N}\sum^{N}(\sin\phi_n - \sin\theta_n)^2 + \frac{1}{N}\sum^{N}(\cos\phi_n - \cos\theta_n)^2\right)} \quad (2)$$

where N is the number of stations, ϕ_n is the direction of the maximum tilt at station n, and θ_n is the direction of maximum tilt from the synthetic source at station n.

[15] In every case, the inflating pipe and crack sources produced polarities opposite the real data at most stations, as did most of the inflating spherical sources. In order for these sources to fit the data, they require deflation prior to the explosion. The inflating spherical source with the lowest RMS error that matched the tilt polarity of the real data at every station is located ~120 m west of the summit at a depth of ~40 m below the surface. This source location is situated between the summit crater and the previously identified VLP source centroid (300 m west and 300 m below the summit crater) [*Lyons and Waite*, 2011] (Figure 3). The location lends some support to the best-fit model despite the high RMS error (0.33), which produces a relatively poor fit to the real data (Figure 3). This discrepancy likely results in part from a tilt signal generated by an extended source and modeling performed assuming a point source. The poor model fit and small number of sources which were able to correctly reproduce the polarity of the real tilt data also indicates that either the model is incapable of reproducing the complex effect of the topography, or that factors other than the topography (e.g., local site effects) also influenced the data. Further use of co-located tilt meters and more sophisticated modeling [e.g., *Maeda et al.*, 2011] will aid in clarifying the contribution of topography to tilt signals.

4. Interpreting Fuego Tilt Cycles

[16] The tilt signals at Fuego show predominately east and south downward tilt beginning ~25 minutes prior to explosions with a reversal in tilt motion several minutes before explosions (Figure 2). This pattern of deformation would seem to indicate deflation followed by a short period of inflation prior to the explosions. However, this conflicts with seismic, SO_2, infrasound, and observations of the explosions [*Lyons and Waite*, 2011; *Nadeau et al.*, 2011], and is seemingly opposite observations of impulsive explosions in other silicic and mafic systems [*Genco and Ripepe*, 2010; *Iguchi et al.*, 2008; *Voight et al.*, 1999, 2000; *Wiens et al.*, 2005]. We attribute this effect to shallow (above the level of the sensors) inflation of the conduit followed by a short period of deflation prior to explosions. The shallow focus of pressurization combines with the steep and irregular topography to produce tilt data reflecting the exact opposite of what would be expected from the process. Modeling of spherical sources beneath symmetric cones with slopes greater than 20° has shown that, at observation distances of less than 3 times the source radius, source inflation will appear as deflation [*Cayol and Cornet*, 1998]. We assume that all our stations are further than three times the source radius from the vent, but it is unknown how irregular topography or a non-spherical or extended source would change this effect.

[17] Inflation – deflation deformation cycles associated with volcanic explosions have been attributed to pressurization of the conduit beneath a degassed and crystallized plug of magma in silicic systems [*Iguchi et al.*, 2008; *Voight et al.*, 1999, 2000], and in mafic systems to gas bubble growth and magma ascent in a relatively open conduit [*Genco and Ripepe*, 2010; *Nishimura*, 2009]. Fuego magmas are basaltic andesites and could conceivably produce the observed tilt signals due to either of these processes, depending on magma supply rate and conduit conditions, which are poorly constrained. However, the duration of the tilt signal, explosion observations, and high infrasound overpressures (>100 Pa at

1 km) suggest that these explosions were not strombolian bubble bursts. *Lyons and Waite* [2011] showed that extensive plagioclase crystallization is expected for Fuego magmas at depths around the best-fit tilt source model due to degassing crystallization, and invoke the destruction of a pressurized plug as the source of the Fuego explosions that produced VLP signals.

[18] The tilt signals at the three stations closest to the summit show that a change in the tilt signal begins several minutes prior to explosions (Figure 2). In the case of strombolian eruptions, the observed change in tilt prior to an explosion can be associated with the ascent of a gas slug above the elevation of the station locations (T. Nishimura, personal communication, 2011). However, based on observations at other volcanoes [e.g., *Iguchi et al.*, 2008] and the characteristics of the explosions and the interpretations of *Lyons and Waite* [2011] and *Nadeau et al.* [2011], we think that the change in tilt polarity just before the explosions is more likely due to gas leaking into preexisting fractures opened in the pressurized conduit wall, or gas escape due to the opening of fractures in the crystallized plug at the top of the conduit. Visual observations of large explosions at Fuego sometimes show a small puff of gas prior to explosions, which may be indicative of this process.

5. Summary

[19] Pre-explosion tilt is derived from the horizontal components of broadband seismometers deployed at Fuego. The tilt sequence shows: 1) slow deformation beginning ~25 minutes prior to explosions, 2) reversal in tilt direction several minutes prior to explosions, and 3) rapid tilting coincident with broadband seismic and infrasound explosion onsets. The steep topography of the upper cone of the volcano appears to significantly affect how the tilt signals are recorded on the horizontal channels. The source location and geometry were constrained using a finite-difference model that includes the 3D topography of Fuego. Best-fit model results place an inflating spherical pressure source centroid ~120 m west and ~40 m below the summit crater. Spherical sources with a flat topography are unable to reproduce the tilt motion and suggest that topography must be considered in order to realistically model deformation source locations and geometry on volcanoes with steep topography. The tilt signals are interpreted as shallow pressure accumulation beneath a plug of degassed magma followed by elastic recovery of deformation coincident with explosive pressure release. The ability to record deformation with portable broadband seismometers aids in unraveling eruption mechanics, especially when combined with other geophysical data.

[20] **Acknowledgments.** We gratefully acknowledge field support from Edgar Barrios, Kyle Brill, Chris Brown, Amilcar Calderas, Gustavo Chigna, Mari Dalton, Jemile Erdem, Tricia Nadeau, Josh Richardson, Jesse Silverman, INGUAT and INSIVUMEH. Thanks to PASSCAL for data acquisition support and equipment. Research and travel was supported by NSF PIRE 0530109. Thanks to Minoru Takeo, Takeshi Nishimura, Rüdiger Escobar, and Bill Rose for stimulating discussions that improved the paper.

[21] The Editor thanks Jeffrey Johnson and an anonymous reviewer for assisting with the evaluation of this paper.

References

Aoyama, H. (2008), Simplified test on tilt response of Cmg40t seismometers [in Japanese with English abstract], *Bull. Volcanol. Soc. Jpn.*, *53*, 35–46.

Aoyama, H., and H. Oshima (2008), Tilt change recorded by broadband seismometer prior to small phreatic explosion of Meakan-Dake volcano, Hokkaido, Japan, *Geophys. Res. Lett.*, *35*, L06307, doi:10.1029/2007GL032988.

Cayol, V., and F. H. Cornet (1998), Effects of topography on the interpretation of the deformation field of prominent volcanoes: Application to Etna, *Geophys. Res. Lett.*, *25*(11), 1979–1982, doi:10.1029/98GL51512.

Chouet, B. A. (1996), New methods and future trends in seismological volcano monitoring, in *Monitoring and Mitigation of Volcano Hazards*, edited by R. Scarpa and R. I. Tilling, pp. 23–97, Springer, Berlin, doi:10.1007/978-3-642-80087-0_2.

Chouet, B., P. Dawson, T. Ohminato, M. Martini, G. Saccorotti, F. Giudicepietro, G. De Luca, G. Milana, and R. Scarpa (2003), Source mechanisms of explosions at Stromboli volcano, Italy, determined from moment-tensor inversions of very-long-period data, *J. Geophys. Res.*, *108*(B1), 2019, doi:10.1029/2002JB001919.

Dawson, P. B., B. A. Chouet, and J. Power (2011), Determining the seismic source mechanism and location for an explosive eruption with limited observational data: Augustine volcano, Alaska, *Geophys. Res. Lett.*, *38*, L03302, doi:10.1029/2010GL045977.

Genco, R., and M. Ripepe (2010), Inflation-deflation cycles revealed by tilt and seismic records at Stromboli volcano, *Geophys. Res. Lett.*, *37*, L12302, doi:10.1029/2010GL042925.

Iguchi, M., H. Yakiwara, T. Tameguri, M. Hendrasto, and J. Hirabayashi (2008), Mechanism of explosive eruption revealed by geophysical observations at the Sakurajima, Suwanosejima and Semeru volcanoes, *J. Volcanol. Geotherm. Res.*, *178*(1), 1–9, doi:10.1016/j.jvolgeores.2007.10.010.

Johnson, J. B., R. Sanderson, J. Lyons, R. Escobar-Wolf, G. Waite, and J. M. Lees (2009), Dissection of a composite volcanic earthquake at Santiaguito, Guatemala, *Geophys. Res. Lett.*, *36*, L16308, doi:10.1029/2009GL039370.

Lyons, J. J., and G. P. Waite (2011), Dynamics of explosive volcanism at Fuego volcano imaged with very long period seismicity, *J. Geophys. Res.*, *116*, B09303, doi:10.1029/2011JB008521.

Maeda, Y., M. Takeo, and T. Ohminato (2011), A waveform inversion including tilt: Method and simple tests, *Geophys. J. Int.*, *184*(2), 907–918, doi:10.1111/j.1365-246X.2010.04892.x.

McTigue, D. F., and P. Segall (1988), Displacements and tilts from dip-slip faults and magma chambers beneath irregular surface topography, *Geophys. Res. Lett.*, *15*(6), 601–604, doi:10.1029/GL015i006p00601.

Meo, M., U. Tammaro, and P. Capuano (2008), Influence of topography on ground deformation at Mt. Vesuvius (Italy) by finite element modelling, *Int. J. Nonlinear Mech.*, *43*(3), 178–186, doi:10.1016/j.ijnonlinmec.2007.12.005.

Mogi, K. (1958), Relations between the eruptions of various volcanoes and the deformations of the ground surface around them, *Bull. Earthquake Res. Inst. Univ. Tokyo*, *36*, 99–134.

Nadeau, P. A., J. L. Palma, and G. P. Waite (2011), Linking volcanic tremor, degassing, and eruption dynamics via SO_2 imaging, *Geophys. Res. Lett.*, *38*, L01304, doi:10.1029/2010GL045820.

Nishimura, T. (2009), Ground deformation caused by magma ascent in an open conduit, *J. Volcanol. Geotherm. Res.*, *187*(3–4), 178–192, doi:10.1016/j.jvolgeores.2009.09.001.

Ohminato, T., and B. A. Chouet (1997), A free-surface boundary condition for including 3D topography in the finite-difference method, *Bull. Seismol. Soc. Am.*, *87*(2), 494–515.

Okada, Y. (1985), Surface deformation due to shear and tensile faults in a half-space, *Bull. Seismol. Soc. Am.*, *75*(4), 1135–1154.

Rodgers, P. W. (1968), The response of the horizontal pendulum seismometer to Rayleigh and Love waves, tilt, and free oscillations of the Earth, *Bull. Seismol. Soc. Am.*, *58*(5), 1385–1406.

Sanderson, R. W., J. B. Johnson, and J. M. Lees (2010), Ultra-long period seismic signals and cyclic deflation coincident with eruptions at Santiaguito volcano, Guatemala, *J. Volcanol. Geotherm. Res.*, *198*(1–2), 35–44, doi:10.1016/j.jvolgeores.2010.08.007.

Voight, B., et al. (1999), Magma flow instability and cyclic activity at Soufriere Hills volcano, Montserrat, British West Indies, *Science*, *283*(5405), 1138–1142, doi:10.1126/science.283.5405.1138.

Voight, B., et al. (2000), Deformation and seismic precursors to dome-collapse and fountain-collapse Nuées Ardentes at Merapi volcano, Java, Indonesia, 1994–1998, *J. Volcanol. Geotherm. Res.*, *100*(1–4), 261–287, doi:10.1016/S0377-0273(00)00140-2.

Waite, G. P., B. A. Chouet, and P. B. Dawson (2008), Eruption dynamics at Mount St. Helens imaged from broadband seismic waveforms: Interaction of the shallow magmatic and hydrothermal systems, *J. Geophys. Res.*, *113*, B02305, doi:10.1029/2007JB005259.

Wielandt, E., and T. Forbriger (1999), Near-field seismic displacement and tilt associated with the explosive activity of Stromboli, *Ann. Geofis.*, *42*, 407–416.

Wiens, D. A., S. H. Pozgay, P. J. Shore, A. W. Sauter, and R. A. White (2005), Tilt recorded by a portable broadband seismograph: The 2003 eruption of Anatahan volcano, Mariana Islands, *Geophys. Res. Lett.*, *32*, L18305, doi:10.1029/2005GL023369.

M. Ichihara, Earthquake Research Institute, University of Tokyo, 1-1-1 Yayoi, Bunkyo-ku, Tokyo 113-0032, Japan. (ichihara@eri.u-tokyo.ac.jp)

J. M. Lees, Department of Geological Sciences, University of North Carolina at Chapel Hill, 313 Mitchell Hall, Chapel Hill, NC 27599, USA. (jonathan.lees@unc.edu)

J. J. Lyons, Instituto Geofisico, Escuela Politecnica Nacional, Ladrón de Guevara E11-253, Aptdo 2759, Quito, Ecuador. (jlyons@igepn.edu.ec)

G. P. Waite, Department of Geological Engineering and Sciences, Michigan Technological University, 1400 Townsend Dr., Houghton, MI 49931, USA. (gpwaite@mtu.edu)